Fabrication of monolithic polymer nanofluidic channels via near-field electrospun nanofibers as sacrificial templates

1 author:

Yiin-Kuen Fuh

National Central University

99 PUBLICATIONS   **1,327** CITATIONS

Some of the authors of this publication are also working on these related projects:

Project   Self-Powered Sensor of highly-aligned piezoelectric fibers View project

Fabrication of monolithic polymer nanofluidic channels via near-field electrospun nanofibers as sacrificial templates

Yiin-Kuen Fuh
Hung-Shuo Hsu

SPIE

Fabrication of monolithic polymer nanofluidic channels via near-field electrospun nanofibers as sacrificial templates

Yiin-Kuen Fuh
Hung-Shuo Hsu
National Central University
Department of Mechanical Engineering
Taoyuan, 32001 Taiwan
E-mail: mikefuh@cc.ncu.edu.tw

Abstract. This paper reports a facile and maskless method for fabricating nanofluidic channel arrays using near-field electrospinning (NFES) templates with prescribed patterns and the polydimethylsiloxane (PDMS) molding technique. Nanochannels were fabricated monolithically through three main steps: 1) direct-writing nanofiber arrays onto a silicon substrate using NFES, 2) PDMS molding of the prescribed nanofibers patterns, and 3) plasma treating PDMS substrate to promote the adhesion and bonding process. The nanochannels fabricated in this study had channel widths ranging from 500 to 1300 nm and depths of 70 to 500 nm, and were patterned in a fashion similar to the wire bonding process routinely used in the semiconductor industry. The nanochannel dimensions were predominantly dictated by electrospun nanofibers, showing that NFES is capable of depositing nanofibers with a diameter down to ~50 nm. Results show that reliable and repeatable nanofluidic channel arrays were speedily fabricated at a very low cost, while nanofluidic patterns and dimensions are predominantly controlled by NFES in a direct-write, addressable manner. © 2011 Society of Photo-Optical Instrumentation Engineers (SPIE). [DOI: 10.1117/1.3644990]

Subject terms: near-field electrospinning; polydimethylsiloxane molding; nanofluidic channel; nanofiber arrays.

Paper 11083R received Jun. 22, 2011; revised manuscript received Aug. 30, 2011; accepted for publication Sep. 12, 2011; published online Oct. 21, 2011.

1 Introduction

Researchers have recently studied nanofabrication and nanofluidic devices in an effort to open a whole new horizon of scientific discovery in nanoscale phenomena. Nanochannels are particularly interesting due to their promising applications. Previous studies focus on nanofluidic channel applications in DNA and protein manipulation, including the denaturation mapping of DNA in nanofluidic channels,[1] entropic unfolding of DNA molecules in nanofluidic channels,[2] field-dependent DNA mobility in nanoslits,[3] and the fabrication of size-controllable nanofluidic channels by nanoimprinting and its application for DNA stretching.[4] Energy conversion in micro/nanosystems is another subject of intense research. Previous efforts to convert hydrostatic energy to electrical power in nanofluidic channels achieved an efficiency of ~3% for a 75-nm high channel.[5,6]

Other studies review the practical fabrication issues of nanochannels, which generally fall into bulk, surface nanomachining, buried channel, and nanoimprint lithography groups.[4,7–9] These four methods suffer from various issues, with shared attributes of extremely high cost and a painstakingly long process. The main cost driver for these fabrication methods is nanolithography, including electron beam lithography,[10] e-beam with ion milling,[11] focused ion beam,[12] or dry etching using nanowire masks. However, these techniques have difficulty producing arbitrary patterns. Atomic force microscope (AFM)-based scanning probe lithography has excellent resolution in terms of fabrication of fluidic channel in nanoscale.[13–16] AFM local-oxidation nanolithography utilizing Mo/PMMA nanomasks and wet chemical etching has been used to fabricate Mn ($Fe_{2.5}Mn_{0.5}O_4$0) thin-film epitaxial nanochannel structures 100-nm wide.[17] Room-temperature ferromagnetism and the potential application of spin-polarized nanoscale circuits holds great promise for spintronics based on nanochannels. Unfortunately, the process of fabricating nanochannel arrays using AFM-based lithography is expensive, complicated, and time-consuming. Previous research proposes a relatively cost-effective, CMOS compatible fabrication technique that uses chemical-mechanical polishing and the thermal oxidation technique without nanolithography.[18] Template-based methods fabricate nanofluidic channels using a combination of various materials, using Ag nanowires (NWs) and ZnO NWs as sacrificial templates. These approaches can produce a monolithic polyimide nanofluidic channel with a diameter of less than 100 nm.[19] Ultraviolet-curable epoxy can replicate an ordered array of nanoscale cracks generated by the mechanical stretching of plasma-oxidized polydimethylsiloxane (PDMS). The negative relief patterns of nanochannels can be obtained by casting PDMS prepolymer against an epoxy mold.[20] Another approach to fabricating site-specific, chip-to-chip fluidic connectors uses near-field electrospinning (NFES).[21–23] In this method, electrospun nanofibers function as sacrificial layers followed by deposition of structural layers and selective etching.[24] The controlled formation of multiple jets and nanofiber deposition using a near-field electrospinning process has been recently demonstrated.[25]

This novel method is suitable for generating templates at high throughput for PDMS molding.

2 Experimental Section

2.1 Electrospinning Solution

The experiments reported in this study used a 8 wt.% polyethylene oxide (PEO) (Mv = 300,000, ECHO Chemical Co., TW) aqueous solution at room temperature and atmospheric pressure after magnetic mixing for 24 h.

2.2 Electrospinning Setup

The proposed approach uses NFES to generate well-aligned and addressable nanofiber arrays. The syringe needle diameter was 400 μm, the needle-to-collector distance was fixed at 500 μm, and the applied voltage was 1100 V. A p-type silicon wafer served as a collector and casting substrate. A high voltage power supply (0 to 15 kV, AU-series, Matsusada Precision Inc.) was used to electrically charge the polymer jet and an optical microscope (ECLIPSE LV150L, Nikon Co.) is used to monitor the fabrication process.

2.3 Molding

The array nanofluidic channel device fabricated on a p-type silicon wafer was used as a master to prepare PDMS (Sylgard 184, Dow Corning) stamps. The components for preparing the elastomers were supplied in two parts: Sylgard-184A and Sylgard-184B. PDMS was first mixed with a curing agent at a volume ratio of 10:1 and placed in vacuum ($\sim$10 Torr) for 30 min to remove any bubbles formed during mixing.

It is essential to remove the air bubbles by proper mixing and desiccators to acquire transparent and defect-free PDMS replicas. Experimental results show that 24 h at room temperature or 1 h at 100°C can provide effective curing. After curing, tweezers were used to peel off the PDMS, which was then cut meticulously using a surgical knife to produce crack-free stamps.

2.4 Bonding

Oxygen plasma treatment is routinely used to covalently bond PDMS to glass. This process is related to the breaking and formation of covalent (Si–O–Si) bonds when the two surfaces are oxidized before mechanical contact.[26–28] Oxygen plasma treatment also makes the channel surfaces more hydrophilic, improving fluid filling. Experimental results show that the surfaces quickly reverted to their hydrophobic tendency when exposed to the atmosphere.[29]

It is very important to maintain the cleanliness of both PDMS stamps and microscope slides before and after the bonding process to create defect-free and well-sealed replications. Oxygen plasma (PDC-32G, Harrick plasma) was used to oxidize both PDMS and slide surfaces before bonding process.

3 Results and Discussion

The experiments in this study successfully and rapidly fabricated array nanofluidic channels using NFES templates with prescribed patterns and the PDMS molding technique. The NFES technique produced micro/nanopolymer patterns at a speed of 20 cm/s, with location controllability better than 20 μm.[20–24] The nanochannel arrays were easily fabricated in
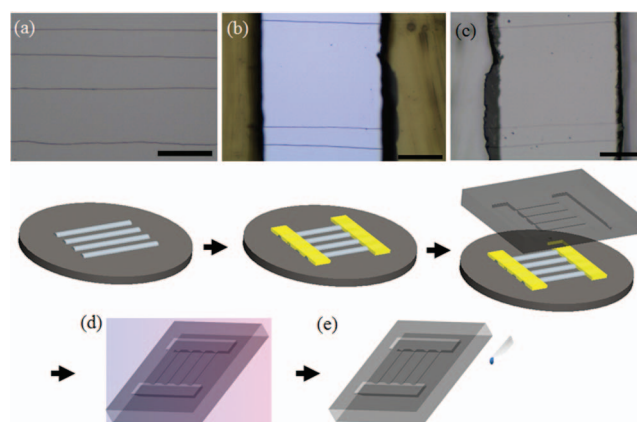

Fig. 1 Schematics and corresponding optical microscope images of each fabrication step of the nanofluidic channel arrays. (a) Direct-writing of multiple nanofibers on silicon (p-type) wafer. (b) Application of Kapton tapes on both sides of nanofiber arrays to create a liquid chamber. (c) PDMS molding of nanofluidic channel arrays. (d) Surface treatment by O$_2$ plasma. (e) Bonding with the same polymer or microscope slide to seal the channel arrays and nanofluidic test. The scale bars in (a), (b), and (c) are 100 μm.

a controlled and maskless manner. Furthermore, we simplify the fabrication process proposed to make suspended fluidic channels via NFES as an application of chip-to-chip fluidic interconnectors.[24] Figure 1 schematically illustrates the fabrication process of nanochannels. First, Fig. 1(a) shows the direct-write, straight, and well-aligned nanofibers on silicon (p-type) wafer. The distance between adjacent nanofibers can be fully controllable from 40 to 150 μm, depending on the stage resolution and vacuum condition. Figure 1(b) shows the capability of adjustable separation from 100 μm to 1 mm using Kapton tapes. Since Kapton tapes also function as liquid chambers, the tape edges were carefully pressed to ensure good bonding interfaces. Figure 1(b) shows that the separation distance is 250 μm. Figure 1(c) shows PDMS molding of templates generated from Fig. 1(b) and casting PDMS in the mold (thickness < 1 mm), followed by vacuum ($\sim$10 Torr) for 15 min to remove excess air bubbles. The final step is hot baking at 100°C for 1 h to completely cure the PDMS. Figure 1(d) illustrates the surface modification process and the O$_2$ plasma (2 min, working pressure of 0.8 Torr) process in particular. To ensure that the surface is hydrophilic, plasma treatment and bonding should be carried out immediately. Bonding with microscope slide and hard-baking (70°C, 5 min) increased the bond strength between the PDMS and slide. Finally, Fig. 1(e) depicts the sealed device ready for the nanofluidic test.

Figure 2(a) shows a schematic illustration of the nanofluidic channel arrays using the proposed method. Figure 2(b) shows an SEM image of three fabricated nanochannels in parallel, where the distances between the adjacent nanochannels are approximately 110 μm (#1 to #2) and 120 μm (#2 to #3). The dimensions and pattern resolution of array nanochannels can be reliably adjustable since the PDMS molding is the replica of NFES counterpart. The following characterization of fiber diameters and standard deviation are calculated based on 20 data points measured directly from SEM in each experiment. Experimentally, when the PEO concentration is 8 wt.%, applied voltage is 1100 V and the needle-to-collector
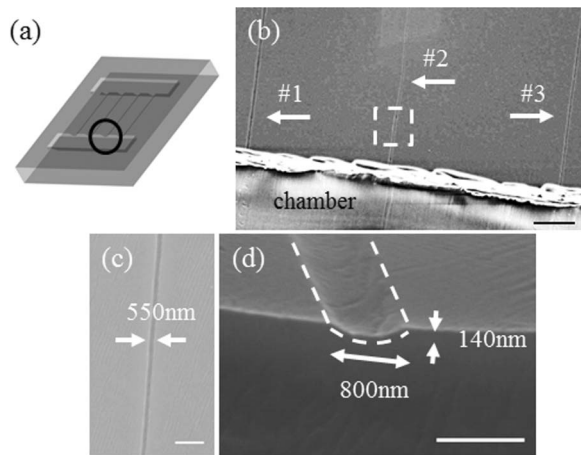
Fig. 2 (a) Schematic illustration of the nanofluidic channel arrays. (b) SEM image of nanochannels and chamber interface. (c) Close-up and sectional view of (b) for nanochannel #2. (d) SEM cross-section for a single nanochannel (800 nm wide, 140 nm deep, semi-elliptical shape). The scale bars in (b), (c), and (d) are 30, 3, and 1 μm, respectively.

Fig. 4 Time-lapse photos showing the liquid front moving through an 800-nm wide nanochannel. (a) 0 s, (b) 2 s, and (c) 7 s.

distance is fixed at 500 μm, the average fiber diameter can be deposited in the range of 490 to 990 nm. After PDMS replication, the semi-elliptical shapes of nanofluidic channels are found to have width distribution between 500 and 1350 nm and depth distribution 100 to 250 nm, respectively. Figure 2(b) demonstrates the fabrication results using the above electrospinning conditions and diameters of electrospun nanofibers range from 490 to 540 nm. Furthermore, the uniformity in the lateral dimension of an individual nanofiber along its longitudinal axis of 100 μm long is experimentally found to be within 8.56% of its diameter (figure not shown here). Figure 2(c) is close-up view of Fig. 2(b), showing a single nanochannel (550 nm wide). Figure 2(d) shows another
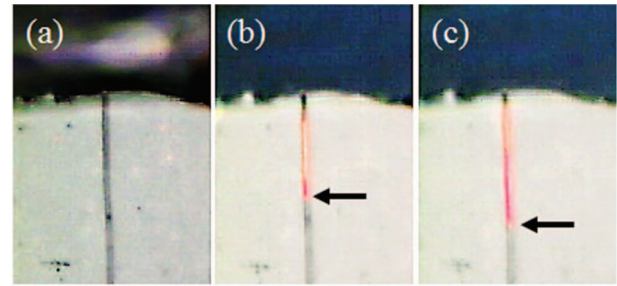
nanochannel in which the width $\times$ depth of the semi-elliptical shape is 800 nm $\times$ 140 nm, corresponding to an aspect ratio (depth/width) of 0.175. The channel depth is not perfectly matched with the electrospun fibers due to mechanical deformation in the PDMS molding process.

Figure 3 shows AFM images of the micro/nanochannels from two different dimensions. Figures 3(a) and 3(b) show two different sizes of 1.3 μm and 500-nm wide micro/nanochannels, respectively. Figures 3(c) and 3(d) show the corresponding three-dimensional AFM images. Figures 3(e) and 3(f) demonstrate the lengthwise depth variations in the transverse section (along the black line). The aspect ratios of these channels can be calculated as 0.185 and 0.14, respectively.

The fabricated PDMS channels were subjected to an initial fluidic test. Figure 4 shows time-lapse photos of the liquid front flowing in a nanochannel. Due to the hydrophilic nature of the plasma-modified surface, deionized water with dye solution can freely pass through the channel without any external force. Figures 4(a)–4(c) show a sequence of time-lapse photos of the dye movement on a nanochannel of 800-nm wide. The flow speed was estimated at 25 μm/s
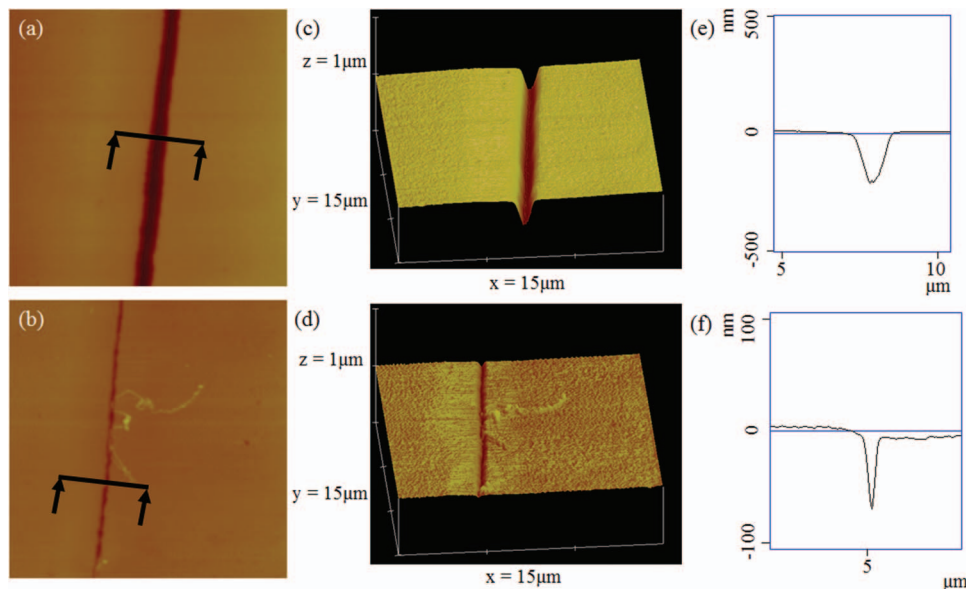

Fig. 3 AFM images (scan area is 15 $\times$ 15 μm^2) and line profiles of nanochannels fabricated via NFES deposited nanofibers as templates. Top view of two different nanochannels measuring (a) 1.3 μm wide and (b) 500 nm wide. Corresponding three-dimensional AFM images of nanochannels for (c) 1.3 μm wide and (d) 500 nm wide. (e) and (f) show line profiles in the transverse section (along the black line) of nanochannels, indicating depths of 240 and 70 nm in (c) and (d), respectively.
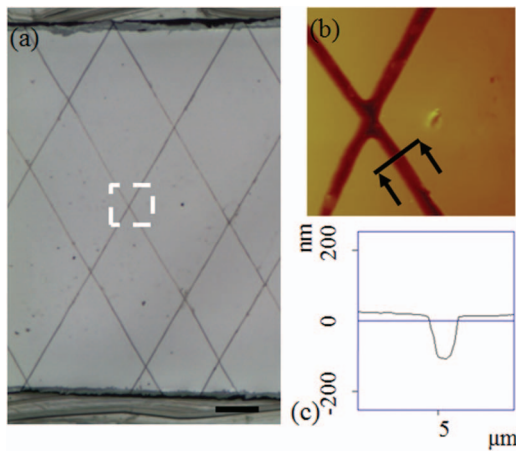
Fig. 5 (a) Optical microscope images of nano/microchannel arrays with cross-linking pattern inclined at approximately 60 deg. The scale bar is 100 μm. (b) Close-up view of (a) an AFM image. (c) Line profiles in the transverse section (along the black line) indicate that the depth in (b) is 130 nm.

initially and 2 μm/s upon reaching the steady state. Previously, capillary force was found to drive liquid inside the silicon dioxide channels with an initial flow speed of 25 μm/s due to the hydrophilic surface.[24] In this study, a similar initial flow speed was found inside PDMS nanochannels, which is consistent with SiO$_2$ nanochannels. On the other hand, the flow speed at the steady state was only 2 μm/s. The exact reason for this significant reduction in flow speed is unclear, but one possible reason may be a lack of driving force to induce the fluid flow.

Figure 5(a) shows an optical microscope image of nano/microchannel arrays with cross-linking pattern inclined at approximately 60 deg. Figure 5(b) shows the corresponding AFM image and Fig. 5(c) demonstrates the lengthwise depth variations of Fig. 5(b) in the transverse section (along the black line), with width × depth ratio of 1.1 μm × 130 nm and an aspect ratio of 0.118. The implication can be the potential integration of nanofluidic channels with site-specific patterns/orientations to serve concurrently as multiple functions such as nanomixers and nanosieves into one fabrication process.[30]

4 Conclusion

This study successfully demonstrates an easy and versatile method of fabricating a monolithic polyimide nanofluidic channel with width × depth dimensions ranging from 500 nm × 70 nm to 1.3 μm × 240 nm. Direct-write electrospun nanofiber arrays served as sacrificial templates. Since the position, diameter, and length of nanofibers can be readily controlled in a fashion analogous to the wire-bonding technique routinely used in microelectronics, the nanochannel geometry and pattern can be easily replicated. Experimental results prove that NFES can produce micro/nanopolymer patterns at a speed of 20 cm/s with location controllability better than 20 μm, and possibly improved to 10 μm using a high resolution motorized stage.[24] Nanochannel arrays can be readily fabricated in a controlled and maskless manner. This novel nanochannel fabrication process is easy and inexpensive compared to conventional fabrication techniques based

on nanolithography, and exhibits a tremendous advantage of "direct assembly" of nanostructures acting as templates.

References

1. W. Reisner, N. B. Larsen, A. Silahtaroglu, A. Kristensen, N. Tommerup, J. O. Tegenfeldt, and H. Flyvbjerg, "Single-molecule denaturation mapping of DNA in nanofluidic channels," *Proc. Natl. Acad. Sci. USA.* **107**, 13294–13299 (2010).
2. S. L. Levy, J. T. Mannion, J. Cheng, C. H. Reccius, and H. G. Craighead, "Entropic unfolding of DNA molecules in nanofluidic channels," *Nano Lett.* **8**, 3839–3844 (2008).
3. G. Salieb-Beugelaar, J. Teapal, J. van Nieuwkasteele, D. Wijnperlé, J. O. Tegenfeldt, F. Lisdat, A. van den Berg, and J. C. T. Eijkel, "Field-dependent DNA mobility in 20 nm high nanoslits," *Nano Lett.* **8**, 1785–1790 (2008).
4. L. J. Guo, X. Cheng, and C. F. Chou, "Fabrication of size-controllable nanofluidic channels by nanoimprinting and its application for DNA stretching," *Nano Lett.* **4**, 69–73 (2004).
5. F. H. J. van der Heyden, D. J. Bonthuis, D. Stein, C. Meyer, and C. Dekker, "Electrokinetic energy conversion efficiency in nanofluidic channels," *Nano Lett.* **6**, 2232–2237 (2006).
6. F. H. J. van der Heyden, D. J. Bonthuis, D. Stein, C. Meyer, and C. Dekker, "Power generation by pressure-driven transport of ions in nanofluidic channels," *Nano Lett.* **7**, 1022–1025 (2007).
7. H. T. Hoang, I. M. Segers-Nolten, J. W. Berenschot, M. J. de Boer, N. R. Tas, J. Haneveld, and M. C. Elwenspoek, "Fabrication and interfacing of nanochannel devices for single-molecule studies," *J. Micromech. Microeng.* **19**, 065017 (2009).
8. J. Perry and S. Kandlikar, "Review of fabrication of nanochannels for single phase liquid flow," *Microfluid. Nanofluid.* **2**, 185–193 (2006).
9. Q. Xia, K. J. Morton, R. H. Austin, and S. Y. Chou, "Sub-10 nm self-enclosed self-limited nanofluidic channel arrays," *Nano Lett.* **8**, 3830–3833 (2008).
10. C. Vieu, F. Carcenac, A. Pépin, Y. Chen, M. Mejias, A. Lebib, L. Manin-Ferlazzo, L. Couraud, and H. Launois, "Electron beam lithography: Resolution limits and applications," *Appl. Surf. Sci.* **164**, 111–117 (2000).
11. O. Céspedes, S. M. Watts, J. M. D. Coey, K. Dorr, and M. Ziese, "Magnetoresistance and electrical hysteresis in stable half-metallic La$_{0.7}$Sr$_{0.3}$MnO$_3$ and Fe$_3$O$_4$ nanoconstrictions," *Appl. Phys. Lett.* **87**, 083102 (2005).
12. T. Arnal, R. Soulimane, A. Aassime, M. Bibes, Ph. Lecoeur, A. M. Haghiri-Gosnet, B. Mercey, A. V. Khvalkovskii, A. K. Zvezdin, and K. A. Zvezdin, "Magnetic nanowires patterned in the La$_{2/3}$Sr$_{1/3}$MnO$_3$ half-metal," *Microelectron. Eng.* **78–79**, 201–205 (2005).
13. R. Garcia, M. Calleja, and H. Rohrer, "Patterning of silicon surfaces with noncontact atomic force microscopy: Field-induced formation of nanometer-size water bridges," *J. Appl. Phys.* **86**, 1898–1903 (1999).
14. E. S. Snow and P. M. Campbell, "AFM fabrication of sub-10-nanometer metal-oxide devices with in situ control of electrical properties," *Science* **270**, 1639–1641 (1995).
15. A. A. Tseng, A. Notargiacomo, and T. P. Chen, "Nanofabrication by scanning probe microscope lithography: A review," *J. Vac. Sci. Technol. B* **23**, 877–894 (2005).
16. I. Song, B. M. Kim, and G. Park, "Fabrication of a josephson junction using an atomic force microscope," *Appl. Phys. Lett.* **76**, 601–603 (2000).
17. L. Pellegrino, Y. Yanagisawa, M. Ishikawa, T. Matsumoto, H. Tanaka, and T. Kawai, "(Fe,Mn)$_3$O$_4$ nanochannels fabricated by AFM local-oxidation nanolithography using Mo/Poly(methyl methacrylate) nanomasks," *Adv. Mater.* **18**, 3099–3104 (2006).
18. C. Lee, E. H. Yang, N. V. Myung, and T. George, "A nanochannel fabrication technique without nanolithography," *Nano Lett.* **3**, 1339–1340 (2003).
19. K. S. Chu, S. Kim, H. Chung, J. H. Oh, T. Y. Seong, B. H. An, Y. K. Kim, J. H. Park, Y. R. Do, and W. Kim, "Fabrication of monolithic polymer nanofluidic channels using nanowires as sacrificial templates," *Nanotechnology* **21**, 425302 (2010).
20. D. Huh, K. L. Mills, X. Zhu, M. A. Burns, M. D. Thouless, and S. Takayama, "Tuneable elastomeric nanochannels for nanofluidic manipulation," *Nat. Mater.* **6**, 424–428 (2007).
21. D. Sun, C. Chang, S. Li, and L. Lin, "Near-field electrospinning," *Nano Lett.* **6**, 839–842 (2006).
22. C. Chang, K. Limkrailassiri, and L. Lin, "Continuous near-field electrospinning for large area deposition of orderly nanofiber patterns," *Appl. Phys. Lett.* **93**, 123111 (2008).

23. C. Chang, V. H. Tran, J. Wang, Y. K. Fuh, and L. Lin, "Direct-write piezoelectric polymeric nanogenerator with high energy conversion efficiency," *Nano Lett.* **10**, 726–731 (2010).
24. S. H. Lee, K. Limkrailassiri, Y. Gao, C. Chang, and L. Lin, "Chip-to-chip fluidic connectors via near-field electrospinning," in *Proceedings of MEMS*, pp. 61–64 (2007).
25. Y. K. Fuh and H. S. Hsu, "Controlled formation of multiple jets and nanofibers deposition via near-field electrospinning process," *Int. J. Nonlinear Sci. Numer. Simul.* **11**, 123–130 (2010).
26. A. Y. N. Sofla and C. Martin, "Study of the vapor-assisted method for bonding PDMS and glass: Effect of the vapor source," *J. Micromech. Microeng.* **20**, 125024 (2010).
27. K. Malecha, I. Gancarz, and W. Tylus, "Argon plasma-assisted PDMS-LTCC bonding technique for microsystem applications," *J. Micromech. Microeng.* **20**, 115006 (2010).
28. J. C. McDonald, D. C. Duffy, J. R. Anderson, D. T. Chiu, H. Wu, O. J. A. Schueller, and G. M. Whitesides, "Fabrication of microfluidic systems in poly(dimethylsiloxane)," *Electrophoresis* **21**, 27–40 (2000).
29. M. A. Eddings, M. A. Johnson, and B. K Gale, "Determining the optimal PDMS-PDMS bonding technique for microfluidic devices," *J. Micromech. Microeng.* **18**, 067001 (2008).
30. Y. Zeng and D. J. Harrison, "Self-assembled colloidal arrays as three-dimensional nanofluidic sieves for separation of biomolecules on microchips," *Anal. Chem.* **79**, 2289–2295 (2007).

Biographies and photographs of the authors not available.